

# Preparation, Crystal Structures, and Isomerization of the Tellurium Diimide Dimers $\text{RNTe}(\mu\text{-NR}')_2\text{TeNR}$ ( $\text{R} = \text{R}' = \text{'Bu}$ ; $\text{R} = \text{PPh}_2\text{NSiMe}_3$ , $\text{R}' = \text{'Bu}$ , $\text{'Oct}$ ): X-ray Structure of the Telluradiazole Dimer [ $\text{'Bu}_2\text{C}_6\text{H}_2\text{N}_2\text{Te}$ ]<sub>2</sub>

Tristram Chivers,\* Xiaoliang Gao, and Masood Parvez

Department of Chemistry, The University of Calgary, Calgary, Alberta, Canada T2N 1N4

Received February 9, 1995<sup>⊗</sup>

The reaction of  $\text{R'NHLi}$  ( $\text{R} = \text{'Bu}$ ,  $\text{'Oct}$ ) with  $\text{Ph}_2\text{P}(\text{NSiMe}_3)_2\text{Te}(\text{Cl})\text{NPPPh}_2\text{NSiMe}_3$  in toluene at  $-78\text{ }^\circ\text{C}$ , followed by warming to  $23\text{ }^\circ\text{C}$ , produces the tellurium diimide dimers  $\text{RNTe}(\mu\text{-NR}')_2\text{TeNR}$  (**2a**,  $\text{R}' = \text{'Bu}$ ,  $\text{R} = \text{NPPPh}_2\text{NSiMe}_3$ ; **2b**,  $\text{R}' = \text{'Oct}$ ,  $\text{R} = \text{NPPPh}_2\text{NSiMe}_3$ ) and  $\text{Ph}_2\text{P}(\text{NHSiMe}_3)(\text{NSiMe}_3)$ . X-ray analyses revealed that **2a** and **2b** have centrosymmetric structures containing a planar four-membered  $\text{Te}_2\text{N}_2$  ring and short exocyclic tellurium–nitrogen bond lengths ( $d(\text{Te}-\text{N}) = 1.900(5)$  and  $1.897(4)$  or  $1.905(4)$  Å for **2a** and **2b**, respectively). The exocyclic imido substituents adopt a *trans* arrangement with respect to the  $\text{Te}_2\text{N}_2$  ring. By contrast, the reaction of  $2,4,6\text{-'Bu}_3\text{C}_6\text{H}_2\text{NHLi}$  with  $\text{Ph}_2\text{P}(\text{NSiMe}_3)_2\text{Te}(\text{Cl})\text{NPPPh}_2\text{NSiMe}_3$  in toluene under similar conditions produces the telluradiazole ( $\text{'Bu}_2\text{C}_6\text{H}_2\text{N}_2\text{Te}$ )<sub>2</sub> (**3**), which exists as a weakly associated dimer in the solid state with intramolecular  $\text{Te}-\text{N}$  distances of  $2.628(4)$  Å. The tellurium diimide dimer  $\text{'BuNTe}(\mu\text{-N'Bu})_2\text{TeN'Bu}$  (**2c'**), prepared by the reaction of  $\text{TeCl}_4$  with  $\text{'BuNHLi}$  in a 1:4 molar ratio, consists of a folded  $\text{Te}_2\text{N}_2$  ring with exocyclic  $\text{N'Bu}$  groups in a *cis* orientation. The  $^1\text{H}$ ,  $^{31}\text{P}$ , and  $^{125}\text{Te}$  NMR spectra of **2a** and **2b** indicate that the *trans* isomers slowly transform into the corresponding *cis* isomers in solution. Crystals of **2b** are triclinic, space group  $P\bar{1}$  (No. 2), with  $a = 13.304(3)$  Å,  $b = 16.927(3)$  Å,  $c = 13.292(5)$  Å,  $\alpha = 98.94(2)$ ,  $\beta = 109.27(2)$ ,  $\gamma = 69.04(2)^\circ$ ,  $V = 2636(1)$  Å<sup>3</sup>, and  $Z = 4$ . The final  $R$  and  $R_w$  values were 0.034 and 0.033, respectively. Crystals of **2c'** are orthorhombic, space group  $Pnma$  (No. 62), with  $a = 9.535(3)$  Å,  $b = 14.264(3)$  Å,  $c = 16.963(4)$  Å,  $V = 2307.1(9)$  Å<sup>3</sup>, and  $Z = 4$ . The final  $R$  and  $R_w$  values were 0.040 and 0.040, respectively. Crystals of **3** are monoclinic, space group  $P2_1/n$  (No. 14), with  $a = 9.117(3)$  Å,  $b = 11.481(4)$  Å,  $c = 16.550(4)$  Å,  $\beta = 97.76(2)^\circ$ ,  $V = 1716.5(8)$  Å<sup>3</sup>, and  $Z = 4$ . The final  $R$  and  $R_w$  values were 0.031 and 0.034, respectively.

## Introduction

Tellurium compounds of the main group elements are attracting attention, in part, as possible precursors to the corresponding tellurides, some of which have desirable properties for applications in the semiconductor industry.<sup>1</sup> In addition, the preparation of multiply bonded tellurium compounds of the p-block elements has represented both a challenge and a source of controversy. Despite considerable efforts, the first telluroketone that is sufficiently stable to be characterized spectroscopically in solution was not reported until 1993.<sup>2</sup> In this context the recent X-ray structural characterization of a terminal germanium(IV) telluride is a remarkable achievement.<sup>3</sup> Although phosphine tellurides  $\text{R}_3\text{PTe}$  have been known for 30 years,<sup>4</sup> the nature of the phosphorus–tellurium bond in these derivatives is still controversial.<sup>5,6</sup> However, these reagents provide a labile source of elemental tellurium in a reactive form and they have been used extensively for the generation of transition-metal–tellurium clusters and, subsequently, the corresponding tellurides.<sup>7</sup>

Compounds containing tellurium–nitrogen double bonds (predicted bond length 1.83 Å) have also proved elusive.<sup>8,9</sup> The

sulfur(IV) diimides  $\text{RN}=\text{S}=\text{NR}$  have been widely studied (a) from the structural viewpoint, (b) as ligands for transition metals, and (c) as reagents in organic synthesis.<sup>10</sup> The corresponding selenium(IV) diimides,  $\text{RN}=\text{Se}=\text{NR}$ , despite a 20 year history,<sup>11</sup> have yet to be structurally characterized in the solid state, presumably owing to their relatively low thermal stability.<sup>12</sup> In recent preliminary communications we have described the preparation and X-ray structural characterization of the first tellurium diimides, which exist as dimers with the exocyclic imido groups in either *trans* (**2a**)<sup>13</sup> or *cis* (**2c'**)<sup>14</sup> orientations with respect to the four-membered  $\text{Te}_2\text{N}_2$  ring. In attempts to kinetically stabilize a monomeric tellurium diimide by the use of very bulky substituents, we have now investigated the reactions of the  $\text{PN}_2\text{Te}$  heterocycle (**1**) (see Scheme 1) with (a)  $\text{'OctNHLi}$  and (b)  $2,4,6\text{-'Bu}_3\text{C}_6\text{H}_2\text{NHLi}$ . The former reagent produces the dimer **2b** whereas the latter unexpectedly yields a telluradiazole, which was shown by X-ray crystallography to exist as the dimer **3** in the solid state. NMR evidence for the presence of both *cis* and *trans* isomers of **2a** and **2b** in solution

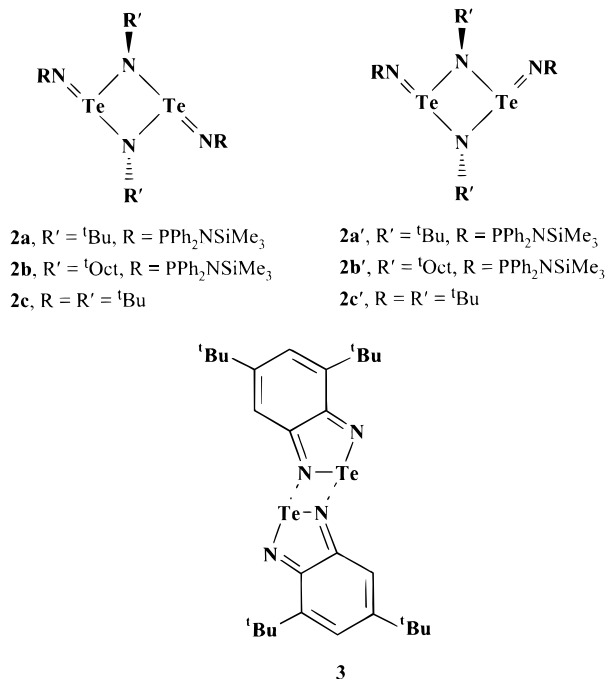
<sup>⊗</sup> Abstract published in *Advance ACS Abstracts*, November 15, 1995.

- Chivers, T. *J. Chem. Soc., Dalton Trans.* **1996**, in press.
- Minoura, M.; Kawashima, T.; Okazaki, R. *J. Am. Chem. Soc.* **1993**, *115*, 7019.
- Kuchta, M.; Parkin, G. *J. Chem. Soc., Chem. Commun.* **1994**, 1351.
- Zingaro, R. A.; Steeves, B. H.; Irgolic, K. *J. Organomet. Chem.* **1965**, *4*, 320.
- Jones, C. H. W.; Sharma, R. D. *Organometallics* **1987**, *6*, 1419.
- Gilheany, D. G. *Chem. Rev.* **1994**, *94*, 1339.
- For examples, see: Steigerwald, M. L.; Siegrist, T.; Stuczynski, S. M.; Kwon, Y.-U. *J. Am. Chem. Soc.* **1992**, *114*, 3155 and references cited therein.

- Münzeberg, J.; Roesky, H. W.; Noltemeyer, M.; Besser, S.; Herbst-Irmer, R. *Z. Naturforsch.* **1993**, *48B*, 199.

- Björqvinnsson, M.; Roesky, H. W. *Polyhedron* **1992**, *10*, 2253.

- For recent examples, see: (a) Anderson, D. G.; Robertson, H. E.; Rankin, D. W. H.; Woollins, J. D. *J. Chem. Soc., Dalton Trans.* **1989**, 859. (b) Pauer, F.; Stalke, D. *J. Organomet. Chem.* **1991**, *418*, 127. (c) Chivers, T.; Hiltz, R. W. *Coord. Chem. Rev.* **1994**, *137*, 201. (d) Hill, A. F. *Adv. Organomet. Chem.* **1994**, *36*, 159.
- Sharpless, K. B.; Hori, T.; Truesdale, L. K.; Dietrich, C. O. *J. Am. Chem. Soc.* **1976**, *98*, 269.
- Wrackmeyer, B.; Distler, B.; Gerstmann, S.; Herberhold, M. *Z. Naturforsch.* **1993**, *48B*, 1307.
- Chivers, T.; Gao, X.; Parvez, M. *J. Chem. Soc., Chem. Commun.* **1994**, 2149.
- Chivers, T.; Gao, X.; Parvez, M. *J. Am. Chem. Soc.* **1995**, *117*, 2359.



is presented. The reactions of 2,4,6-<sup>t</sup>Bu<sub>3</sub>C<sub>6</sub>H<sub>2</sub>NHLi and EtNHLi with TeCl<sub>4</sub> were also investigated.

### Experimental Section

The compound Ph<sub>2</sub>P(NSiMe<sub>3</sub>)<sub>2</sub>Te(Cl)NPPPh<sub>2</sub>NSiMe<sub>3</sub> was prepared from Li[Ph<sub>2</sub>P(NSiMe<sub>3</sub>)<sub>2</sub>] and TeCl<sub>4</sub> in a 2:1 molar ratio by the literature procedure.<sup>15</sup> The dimer <sup>t</sup>BuNTe(μ-N<sup>t</sup>Bu)<sub>2</sub>TeN<sup>t</sup>Bu was obtained by the reaction of TeCl<sub>4</sub> with <sup>t</sup>BuNHLi (1:4 molar ratio) as described in ref 14. TeCl<sub>4</sub> and 2,4,6-<sup>t</sup>Bu<sub>3</sub>C<sub>6</sub>H<sub>2</sub>NH<sub>2</sub> (Aldrich) were used as received. The primary amines RNH<sub>2</sub> (R = <sup>t</sup>Bu, <sup>t</sup>Oct) were obtained from Aldrich and dried over molecular sieves before treatment with <sup>n</sup>BuLi (Aldrich) to give the RNHLi reagents. Solvents were dried with the appropriate drying agents and distilled immediately before use. All reactions and the manipulation of air-sensitive products were carried out under an atmosphere of argon.

<sup>1</sup>H NMR spectra were recorded on a Bruker ACE 200 spectrometer, and chemical shifts are reported relative to Me<sub>4</sub>Si in CDCl<sub>3</sub>. <sup>31</sup>P and <sup>125</sup>Te NMR spectra were obtained by use of a Bruker AM-400 spectrometer, and chemical shifts are reported with reference to external 85% H<sub>3</sub>PO<sub>4</sub> and K<sub>2</sub>TeO<sub>3</sub> in D<sub>2</sub>O, respectively. Infrared spectra were obtained as Nujol mulls on a Mattson 4030 FTIR spectrophotometer. Elemental analyses were provided by the Analytical Services Laboratory, Department of Chemistry, University of Calgary.

**Preparation of RNTe(μ-N<sup>t</sup>Bu)<sub>2</sub>TeNR (R = PPh<sub>2</sub>NSiMe<sub>3</sub>) (2a).** A solution of <sup>t</sup>BuNHLi (0.047 g, 0.585 mmol) in toluene (1 mL) was added slowly to a solution of Ph<sub>2</sub>P(NSiMe<sub>3</sub>)<sub>2</sub>Te(Cl)NPPPh<sub>2</sub>NSiMe<sub>3</sub>·0.5C<sub>7</sub>H<sub>8</sub> (0.500 g, 0.585 mmol) in toluene (30 mL) at -78 °C with stirring. The mixture was allowed to warm slowly to 23 °C to give an orange solution. The <sup>31</sup>P NMR spectrum of the reaction mixture showed a singlet at -0.03 ppm attributed to Ph<sub>2</sub>P(NSiMe<sub>3</sub>)(NHSiMe<sub>3</sub>) (lit.: δ(<sup>31</sup>P) (in CDCl<sub>3</sub>) +0.2).<sup>16</sup> The intensity of this signal was equal to the combined intensities of the resonances for **2a** and **2a'** (see Table 1). Removal of the solvent under vacuum produced orange crystals which were washed with cold (-78 °C) hexane (2 × 10 mL) to give **2a** (0.261 g, 0.534 mmol, 92% yield). Anal. Calcd for C<sub>19</sub>H<sub>28</sub>N<sub>3</sub>PSiTe: C, 46.94; H, 5.80; N, 8.64. Found: C, 47.04; H, 5.57; N, 9.06. Solutions of **2a** were shown by <sup>1</sup>H, <sup>31</sup>P, and <sup>125</sup>Te NMR to slowly produce another isomer **2a'** over a period of several hours at room temperature. The NMR data for both isomers are summarized in Table 1.

### Scheme 1

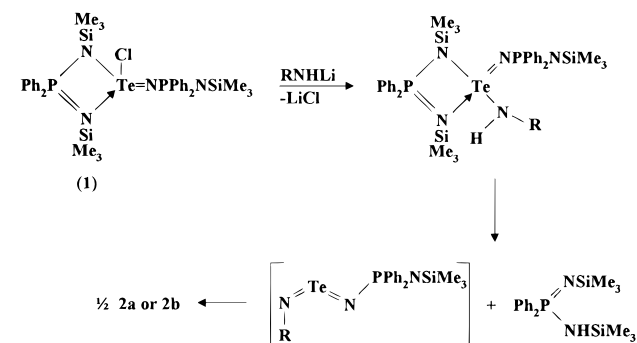


**Table 1.** Spectroscopic Data for **2a**, **2a'**, **2b**, and **2b'**<sup>a</sup>

	δ( <sup>31</sup> P) <sup>b,c</sup>	δ( <sup>125</sup> Te) <sup>b,d</sup>	<sup>2</sup> J( <sup>31</sup> P- <sup>125</sup> Te) <sup>e</sup>	δ( <sup>1</sup> H) <sup>f</sup>
<b>2a</b>	14.4	1808.2 (d)	131.2	7.9–8.1 (m, C <sub>6</sub> H <sub>5</sub> ) 7.0–7.2 (m, C <sub>6</sub> H <sub>5</sub> ) 1.069 (s, C(CH <sub>3</sub> ) <sub>3</sub> ) 0.277 (s, Si(CH <sub>3</sub> ) <sub>3</sub> )
<b>2a'</b> <sup>g</sup>	12.5	1632.4 (d)	109.2	7.9–8.1 (m, C <sub>6</sub> H <sub>5</sub> ) 7.0–7.2 (m, C <sub>6</sub> H <sub>5</sub> ) 1.073 (s, C(CH <sub>3</sub> ) <sub>3</sub> ) 0.369 (s, Si(CH <sub>3</sub> ) <sub>3</sub> )
<b>2b</b>	14.2	1663.8 (d)	128.0	8.0–8.14 (m, C <sub>6</sub> H <sub>5</sub> ) 7.02–7.2 (m, C <sub>6</sub> H <sub>5</sub> ) 1.73 (d, CH) <sup>h</sup> 1.51 (d, CH) <sup>h</sup> 1.29 (s, CH <sub>3</sub> ) 1.17 (s, CH <sub>3</sub> ) 0.81 (s, C(CH <sub>3</sub> ) <sub>3</sub> ) 0.33 (s, Si(CH <sub>3</sub> ) <sub>3</sub> )
<b>2b'</b> <sup>g</sup>	12.9	1806.0 (d)	137.0	<i>i</i>

<sup>a</sup> s = singlet, d = doublet, m = multiplet. <sup>b</sup> In THF at 25 °C. <sup>c</sup> In ppm relative to external 85% H<sub>3</sub>PO<sub>4</sub>. <sup>d</sup> In ppm relative to external K<sub>2</sub>TeO<sub>3</sub> in D<sub>2</sub>O. <sup>e</sup> In Hz. <sup>f</sup> In C<sub>6</sub>D<sub>6</sub> at 25 °C. <sup>g</sup> **2a'** and **2b'** are the isomers of **2a** and **2b**, respectively, that are formed in solution (see text). <sup>h</sup> <sup>2</sup>J(HH) = 14.08 Hz. <sup>i</sup> Not determined due to overlap of resonances with those of **2b**.

**Preparation of RNTe(μ-N<sup>t</sup>Oct)<sub>2</sub>TeNR (R = PPh<sub>2</sub>NSiMe<sub>3</sub>) (2b).** The *tert*-octyl derivative **2b** was obtained as orange crystals in 84% yield from Ph<sub>2</sub>P(NSiMe<sub>3</sub>)<sub>2</sub>Te(Cl)NPPPh<sub>2</sub>NSiMe<sub>3</sub> and <sup>t</sup>OctNHLi by a procedure similar to that described for **2a**. Anal. Calcd for C<sub>23</sub>H<sub>36</sub>N<sub>3</sub>PSiTe: C, 51.04; H, 6.70; N, 7.76. Found: C, 51.27; H, 6.83; N, 7.54. The dimer **2b** also isomerizes in THF solution at room temperature. The NMR data for the two isomers **2b** and **2b'** are summarized in Table 1.

**Preparation of (C<sub>6</sub>H<sub>2</sub>Bu<sub>2</sub>N<sub>2</sub>Te)<sub>2</sub> (3).** A solution of 2,4,6-<sup>t</sup>Bu<sub>3</sub>C<sub>6</sub>H<sub>2</sub>NHLi·Et<sub>2</sub>O (0.341 g, 1.00 mmol) in toluene (30 mL) was added slowly to a solution of Ph<sub>2</sub>P(NSiMe<sub>3</sub>)<sub>2</sub>TeCl(NPPPh<sub>2</sub>NSiMe<sub>3</sub>)·0.5C<sub>7</sub>H<sub>8</sub> (0.855 g, 1.00 mmol) in toluene (30 mL) at -100 °C. The reaction mixture was allowed to warm slowly to room temperature, and the solution changed from colorless to dark orange, followed by green and, finally, red-orange. The <sup>31</sup>P NMR spectrum of the reaction mixture showed a singlet at 0.02 ppm, attributed to Ph<sub>2</sub>P(NSiMe<sub>3</sub>)(NHSiMe<sub>3</sub>) and five other singlets at 36.3, 24.4, 11.1, -1.6, and -4.1 ppm. Solvent was removed under vacuum, and the residue was dissolved in acetonitrile (3 mL). After 24 h at -20 °C, the supernatant was decanted and the remaining solid was recrystallized from pentane to give orange crystals of (C<sub>6</sub>H<sub>2</sub>Bu<sub>2</sub>N<sub>2</sub>Te)<sub>2</sub> (0.141 g, 0.41 mmol, 41%); mp 207–208 °C. Anal. Calcd for C<sub>14</sub>H<sub>20</sub>N<sub>2</sub>Te: C, 48.89; H, 5.86; N, 8.14. Found: C, 49.10; H, 6.01; N, 7.93. <sup>1</sup>H NMR (in C<sub>6</sub>D<sub>6</sub>, δ): 7.62 (d, <sup>4</sup>J<sub>HH</sub> = 2.06 Hz, 1H), 7.36 (d, <sup>4</sup>J<sub>HH</sub> = 2.06 Hz, 1H), 1.78 (s, 9H), 1.30 (s, 9H).

**X-ray Analyses.** **2b.** A suitable orange crystal of RNTe(μ-N<sup>t</sup>Oct)<sub>2</sub>TeNR (R = PPh<sub>2</sub>NSiMe<sub>3</sub>) with dimensions 0.40 × 0.45 × 0.60 mm was obtained from hexane at 23 °C and mounted in a glass capillary. Accurate cell dimensions and a crystal orientation matrix were obtained on a Rigaku AFC6S diffractometer by a least-squares fit of the setting angles of 15 reflections with 2θ in the range 20–40°. Intensity data were collected at -53 °C by the ω/2θ method using a

(15) Chivers, T.; Doxsee, D. D.; Gao, X.; Parvez, M. *Inorg. Chem.* **1994**, *33*, 5678.

(16) Chivers, T.; Dhathathreyan, K. S.; Liblong, S. W.; Parks, T. *Inorg. Chem.* **1988**, *27*, 1305.

**Table 2.** Crystallographic Data for  $RNTe(\mu-N^iOct)_2NR$  ( $R = PPh_2NSiMe_3$ ) (**2b**),  ${}^iBuNTe(\mu-N^iBu)_2TeN^iBu$  (**2c'**), and  $({}^iBu_2C_6H_2N_2Te)_2$  (**3**)

	<b>2b</b>	<b>2c'</b>	<b>3</b>
formula	$(C_{23}H_{36}N_3SiPTe)_2$	$C_{16}H_{36}N_4Te_2$	$(C_{14}H_{20}N_2Te)_2 \cdot C_5H_{12}$
fw	1082.44	539.69	760.00
space group	$P\bar{1}$ (No. 2)	$Pnma$ (No. 62)	$P2_1/n$ (No. 14)
$a$ , Å	13.304(3)	9.535(3)	9.117(3)
$b$ , Å	16.927(3)	14.264(3)	11.481(4)
$c$ , Å	13.292(5)	16.963(4)	16.550(4)
$\alpha$ , deg	98.94(2)		
$\beta$ , deg	109.27(2)		97.76(2)
$\gamma$ , deg	69.04(2)		
$V$ , Å <sup>3</sup>	2636(1)	2307.1(9)	1716.5(8)
$Z$	2	4	2
$T$ , °C	-53.0	23.0	-123.0
$\lambda$ , Å	0.710 69	0.710 69	0.710 69
$\rho_{\text{calcd}}$ , g cm <sup>-3</sup>	1.364	1.554	1.470
$\mu$ , cm <sup>-1</sup>	12.48	25.33	17.26
$R^a$	0.034	0.040	0.031
$R_w^b$	0.033	0.040	0.034

$$^a R = \sum ||F_o| - |F_c|| / \sum |F_o|, \quad ^b R_w = [\sum w\delta^2 / \sum wF_o^2]^{1/2}.$$

scan speed of 16.0° min<sup>-1</sup>, scan width (1.84 + 0.34 tan  $\theta$ )°, and monochromated Mo K $\alpha$  radiation in the range 4.0° < 2 $\theta$  < 50.2°.

The intensities of 9338 reflections were measured, of which 6289 had  $I > 3\sigma(I)$ . Data were corrected for Lorentz, polarization, and absorption effects.<sup>17</sup> Crystal data are given in Table 2, and positional parameters are reported in Table 3. The structure was solved and expanded by using Fourier techniques.<sup>18</sup> The non-hydrogen atoms were refined anisotropically. Hydrogen atoms were included but not refined. Refinement converged with  $R = 0.034$  and  $R_w = 0.033$ . For all three structures, scattering factors were those of Cromer and Waber,<sup>19</sup> and allowance was made for anomalous dispersion.<sup>20</sup>

**2c'**. A orange block (0.30 × 0.33 × 0.40 mm) of  ${}^iBuNTe(\mu-N^iBu)_2TeN^iBu$  was obtained by sublimation at 75 °C/10<sup>-4</sup> Torr. Accurate cell dimensions and a crystal orientation matrix were obtained on a Rigaku AFC6S diffractometer by a least-squares fit of the setting angles of 25 reflections in the range 15–40°. Intensity data were collected at 23 °C by the  $\omega/2\theta$  method using a scan speed of 16.0° min<sup>-1</sup>, scan width (1.73 + 0.34 tan  $\theta$ )°, and monochromated Mo K $\alpha$  radiation in the range 6.0° < 2 $\theta$  < 50.1°.

The intensities of 2354 reflections were measured, of which 942 had  $I > 3\sigma(I)$ . Data were corrected for Lorentz, polarization, and absorption effects.<sup>17</sup> Crystal data are given in Table 2, and positional parameters are reported in Table 4. The structure was solved by direct methods<sup>21</sup> and expanded using Fourier techniques.<sup>18</sup> The non-hydrogen atoms were refined anisotropically. Hydrogen atoms were included by not refined. Refinement converged with  $R = 0.40$  and  $R_w = 0.040$ .

**3**. An orange plate (0.82 × 0.53 × 0.23 mm) of  ${}^iBu_2C_6H_2N_2Te \cdot 0.5C_5H_{12}$  was obtained from pentane solution at 23 °C. Accurate cell dimensions and a crystal orientation matrix were obtained on a Rigaku AFC6S diffractometer by a least-squares fit of the setting angles of 25 reflections with 2 $\theta$  in the range 20–30°. Intensity data were collected at -123 °C by the  $\omega/2\theta$  method using a scan speed of 16.0° min<sup>-1</sup>, scan width (1.63 + 0.34 tan  $\theta$ )°, and monochromated Mo K $\alpha$  radiation in the range 4.0° < 2 $\theta$  < 60°.

The intensities of 5266 reflections were measured, of which 3401 had  $I > 3\sigma(I)$ . Data were corrected for Lorentz, polarization, and

**Table 3.** Atomic Coordinates and  $B_{\text{eq}}$  Values for **2b**

atom	$x$	$y$	$z$	$B_{\text{eq}}, \text{Å}^2$
Te(1a)	0.93938(3)	0.48244(2)	0.07430(3)	2.200(9)
Te(1b)	1.09894(3)	0.97629(2)	0.44826(3)	2.393(10)
P(1a)	0.7756(1)	0.58998(9)	0.1869(1)	2.36(3)
P(1b)	1.1800(1)	0.84784(9)	0.2909(1)	2.35(3)
Si(1a)	0.8312(2)	0.4322(1)	0.3143(1)	3.57(4)
Si(1b)	1.3405(1)	0.9493(1)	0.3289(1)	3.29(4)
N(1a)	0.8497(4)	0.5917(3)	0.1105(3)	2.7(1)
N(1b)	1.1005(4)	0.8711(3)	0.3719(3)	2.6(1)
N(2a)	0.9215(3)	0.4917(3)	-0.0813(3)	2.4(1)
N(2b)	0.9338(4)	1.0461(3)	0.4224(3)	2.7(1)
N(3a)	0.7945(4)	0.5027(3)	0.2225(4)	3.2(1)
N(3b)	1.2283(4)	0.9163(3)	0.2809(4)	3.1(1)
C(1a)	0.8017(5)	0.6683(3)	0.2921(4)	2.5(1)
C(1b)	1.2858(4)	0.7454(3)	0.3351(4)	2.3(1)
C(2a)	0.7328(5)	0.7011(4)	0.3582(5)	3.7(2)
C(2b)	1.2854(4)	0.7045(4)	0.4164(5)	3.4(2)
C(3a)	0.7548(6)	0.7602(4)	0.4393(5)	4.4(2)
C(3b)	1.3714(6)	0.6303(4)	0.4527(5)	4.6(2)
C(4a)	0.8432(6)	0.7884(4)	0.4545(5)	4.2(2)
C(4b)	1.4556(5)	0.5967(4)	0.4064(6)	4.4(2)
C(5a)	0.9127(6)	0.7576(4)	0.3911(5)	4.3(2)
C(5b)	1.4559(5)	0.6354(4)	0.3232(6)	4.1(2)
C(6a)	0.8904(5)	0.6970(4)	0.3096(5)	3.6(2)
C(6b)	1.3711(5)	0.7102(4)	0.2885(4)	3.4(2)
C(7a)	0.6290(5)	0.6378(3)	0.1122(4)	2.6(1)
C(7b)	1.0915(5)	0.8233(3)	0.1613(4)	2.6(1)
C(8a)	0.5544(6)	0.5948(4)	0.0874(6)	4.6(2)
C(8b)	1.0337(5)	0.7675(4)	0.1497(5)	3.2(1)
C(9a)	0.4422(7)	0.6307(6)	0.0292(6)	6.2(2)
C(9b)	0.9676(5)	0.7487(4)	0.0513(5)	3.7(2)
C(10a)	0.4043(6)	0.7113(6)	-0.0006(6)	6.3(2)
C(10b)	0.9593(6)	0.7853(5)	-0.0372(5)	5.2(2)
C(11a)	0.4773(7)	0.7555(5)	0.0212(6)	6.2(2)
C(11b)	1.0142(7)	0.8415(6)	-0.0278(5)	6.3(2)
C(12a)	0.5902(6)	0.7188(4)	0.0775(5)	4.7(2)
C(12b)	1.0819(6)	0.8609(5)	0.0710(5)	4.8(2)
C(13a)	0.9598(9)	0.3462(7)	0.3099(9)	15.0(4)
C(13b)	1.4151(7)	0.9228(6)	0.4727(6)	7.9(3)
C(14a)	0.7178(9)	0.3850(6)	0.2861(8)	11.1(4)
C(14b)	1.4449(7)	0.9046(5)	0.2547(7)	7.3(3)
C(15a)	0.8449(9)	0.4790(6)	0.4510(6)	10.0(3)
C(15b)	1.2890(6)	1.0661(4)	0.3156(6)	5.8(2)
C(16a)	0.8104(5)	0.5198(4)	-0.1657(4)	2.7(1)
C(16b)	0.8480(5)	1.0675(3)	0.3155(4)	2.9(1)
C(17a)	0.7344(5)	0.4806(4)	-0.1416(5)	3.9(2)
C(17b)	0.9087(5)	1.0881(4)	0.2487(5)	4.3(2)
C(18a)	0.8333(5)	0.4791(4)	-0.2709(5)	4.1(2)
C(18b)	0.7550(5)	1.1469(4)	0.3335(5)	4.4(2)
C(19a)	0.7665(5)	0.6180(4)	-0.1621(4)	2.9(1)
C(19b)	0.8081(5)	0.9904(3)	0.2969(4)	2.9(1)
C(20a)	0.6598(5)	0.6732(4)	-0.2440(5)	3.7(2)
C(20b)	0.7154(5)	0.9882(4)	0.1635(4)	3.5(2)
C(21a)	0.5551(6)	0.6516(5)	-0.2589(6)	5.9(2)
C(21b)	0.7430(7)	1.0043(5)	0.0670(5)	6.3(2)
C(22a)	0.6394(6)	0.7646(4)	-0.1990(6)	5.8(2)
C(22b)	0.5989(6)	1.0488(4)	0.1655(6)	5.9(2)
C(23a)	0.6770(7)	0.6706(6)	-0.3520(6)	8.2(3)
C(23b)	0.7078(5)	0.8985(4)	0.1486(5)	5.0(2)

$$^a B_{\text{eq}} = \frac{8}{3}\pi^2(U_{11}(aa^*)^2 + U_{22}(bb^*)^2 + U_{33}(cc^*)^2 + 2U_{12}aa^*bb^* \cos \gamma + 2U_{13}aa^*cc^* \cos \beta + 2U_{23}bb^*cc^* \cos \alpha).$$

(17) North, A. C. T.; Phillips, D. C.; Mathews, F. S. *Acta Crystallogr.* **1968**, A24, 351.

(18) DIRDIF92: Beurskens, P. T.; Admiraal, G.; Beurskens, G.; Bosman, W. P.; Garcia-Granda, S.; Gould, R. O.; Smits, J. M. M.; Smykalla, C. The DIRDIF program system. Technical Report; Crystallography Laboratory, University of Nijmegen: Nijmegen, The Netherlands, 1992.

(19) Cromer, D. T.; Waber, J. T. *International Tables for Crystallography*; Kynoch Press: Birmingham, England, 1974; Vol. IV, Table 2.2A, pp 71–98.

(20) Cromer, D. T.; Liberman, D. J. *Chem. Phys.* **1970**, 53, 1891.

(21) SIR92: Altomare, A.; Burla, M. C.; Camalli, M.; Cascarano, M.; Giacovazzo, C.; Guagliardi, A.; Polidori, G. *J. Appl. Crystallogr.*, in preparation.

absorption effects.<sup>17</sup> Crystal data are given in Table 2, and positional parameters are reported in Table 5. The structure was solved by direct methods<sup>22</sup> and expanded using Fourier techniques.<sup>18</sup> The non-hydrogen atoms were refined anisotropically. A molecule of pentane was located on an inversion center and was found to be disordered. Hydrogen atoms were included but not refined; H atoms of the pentane solvate were ignored. Refinement converged with  $R = 0.031$  and  $R_w = 0.034$ . All calculations were performed using TEXSAN.<sup>23</sup>

(22) SAPI91: Fan Hai-Fu. *Structure Analysis Programs with Intelligent Control*; Rigaku Corp.: Tokyo, 1991.

**Table 4.** Atomic Coordinates and  $B_{\text{eq}}$  Values for  $({}^1\text{Bu}_2\text{C}_6\text{H}_2\text{N}_2\text{Te})_2$  (3)

atom	x	y	z	$B_{\text{eq}}, \text{\AA}^2$
Te(1)	0.32015(3)	0.05269(3)	0.03435(2)	1.609(6)
N(1)	0.1710(4)	0.1588(3)	-0.0281(2)	1.59(7)
N(2)	0.4372(4)	0.0733(3)	-0.0586(2)	1.52(8)
C(1)	0.3636(5)	0.1428(4)	-0.1134(2)	1.31(8)
C(2)	0.2188(5)	0.1888(4)	-0.0978(2)	1.27(9)
C(3)	0.1348(5)	0.2630(4)	-0.1592(2)	1.33(9)
C(4)	0.1987(5)	0.2870(4)	-0.2274(2)	1.50(9)
C(5)	0.3429(5)	0.2441(4)	-0.2425(2)	1.36(9)
C(6)	0.4221(4)	0.1743(4)	-0.1872(2)	1.33(9)
C(7)	-0.0167(5)	0.3105(4)	-0.1468(2)	1.51(9)
C(8)	-0.0862(5)	0.3818(4)	-0.2209(3)	2.0(1)
C(9)	-0.1226(5)	0.2104(4)	-0.1352(3)	2.1(1)
C(10)	-0.0004(5)	0.3908(4)	-0.0715(3)	2.0(1)
C(11)	0.3970(5)	0.2832(4)	-0.3226(2)	1.53(9)
C(12)	0.4120(6)	0.4167(4)	-0.3229(3)	2.6(1)
C(13)	0.2852(5)	0.2453(5)	-0.3956(3)	2.5(1)
C(14)	0.5466(5)	0.2296(4)	-0.3326(3)	2.0(1)
C(15)	1.0000	0.0000	0.5000	3.6(2)
C(16a)	1.0741(12)	-0.0903(10)	0.4658(7)	3.5(3)
C(16b)	0.9658(12)	-0.0026(10)	0.5893(7)	3.3(3)
C(17)	1.1023(7)	-0.0909(6)	0.3776(4)	4.8(2)

$${}^a B_{\text{eq}} = \frac{8}{3}\pi^2(U_{11}(aa^*)^2 + U_{22}(bb^*)^2 + U_{33}(cc^*)^2 + 2U_{12}aa^*bb^* \cos \gamma + 2U_{13}aa^*cc^* \cos \beta + 2U_{23}bb^*cc^* \cos \alpha).$$

**Table 5.** Selected Bond Distances (Å) and Bond Angles (deg) for **2b**<sup>a</sup>

	molecule A	molecule B
Te(1a)–N(1a)	1.897(4)	1.905(4)
Te(1a)–N(2a)	2.027(4)	2.028(4)
Te(1a)–N(2a)*	2.019(4)	2.025(4)
N(1a)–P(1a)	1.642(4)	1.660(4)
P(1a)–N(3a)	1.530(4)	1.553(4)
N(3a)–Si(1a)	1.673(5)	1.675(4)
N(2a)–C(16a)	1.496(6)	1.500(6)
P(1a)–C(1a)	1.807(5)	1.832(5)
P(1a)–C(7a)	1.813(6)	1.821(5)
Si(1a)–C(13a)	1.818(8)	1.881(7)
Si(1a)–C(14a)	1.857(9)	1.842(7)
Si(1a)–C(15a)	1.843(8)	1.862(7)
N(2a)–Te(1a)–N(2a)*	77.1(2)	77.4(2)
N(1a)–Te(1a)–N(2a)	102.6(2)	105.5(2)
N(1a)–Te(1a)–N(2a)*	99.5(2)	98.1(2)
Te(1a)–N(2a)–Te(1a)*	102.9(2)	102.6(2)
Te(1a)–N(2a)–C(16a)	124.2(3)	125.8(3)
Te(1a)*–N(2a)–C(16a)	125.4(3)	124.6(3)
Te(1a)–N(1a)–P(1a)	113.4(2)	111.1(2)
N(1a)–P(1a)–N(3a)	115.9(2)	117.1(2)
P(1a)–N(3a)–Si(1a)	153.4(3)	143.7(3)
N(1a)–P(1a)–C(1a)	103.7(2)	103.8(2)
N(3a)–P(1a)–C(1a)	116.2(2)	115.0(2)
N(1a)–P(1a)–C(7a)	106.1(2)	105.1(2)
N(3a)–P(1a)–C(7a)	110.1(3)	110.2(3)
C(1a)–P(1a)–C(7a)	103.7(2)	104.3(2)

<sup>a</sup> Atoms related by symmetry operations. Molecule A: 2 – x, 1 – y, –z. Molecule B: 2 – x, 2 – y, 1 – z.

## Results and Discussion

**Synthesis of  $\text{RNTe}(\mu\text{-NR}')_2\text{TeNR}$  (**2a**,  $\text{R}' = {}^1\text{Bu}$ ,  $\text{R} = \text{PPh}_2\text{NSiMe}_3$ ; **2b**,  $\text{R}' = {}^i\text{Oct}$ ,  $\text{R} = \text{PPh}_2\text{NSiMe}_3$ ).** The reaction of  $\text{Ph}_2\text{P}(\text{NSiMe}_3)_2\text{Te}(\text{Cl})\text{NPPH}_2\text{NSiMe}_3$  (**1**) with  $\text{RNHLi}$  ( $\text{R} = {}^1\text{Bu}$ ,  ${}^i\text{Oct}$ ) in toluene at  $-78^\circ\text{C}$ , followed by warming to room temperature, produces **2a** and **2b** as thermally stable, extremely moisture-sensitive crystals. As indicated in Scheme 1, this reaction proceeds by the replacement of  $\text{Cl}^-$  in **1** by an amido ligand followed by elimination of  $\text{Ph}_2\text{P}(\text{NSiMe}_3)(\text{NHSiMe}_3)$  (detected by  ${}^{31}\text{P}$  NMR spectroscopy) to give the putative

tellurium diimide monomers  $\text{RNTeNPPH}_2\text{NSiMe}_3$ , which dimerize immediately to give **2a** and **2b** in 90–95% yields; i.e., dimerization occurs to give four-membered  $\text{Te}_2\text{N}_2$  ring with NR ( $\text{R} = {}^1\text{Bu}$ ,  ${}^i\text{Oct}$ ) groups occupying the bridging positions exclusively.

The diimides  $\text{RN}=\text{E}=\text{NR}$  ( $\text{E} = \text{S}, \text{Se}$ ) can be conveniently prepared by treatment of primary amines with sulfur(IV)<sup>24</sup> or selenium(IV)<sup>11,12</sup> halides. The successful, albeit unexpected, generation of thermally stable tellurium diimides by the route depicted in Scheme 1 prompted an investigation of the preparation of  $N,N'$ -diorgano tellurium diimides with bulky organic substituents. In this context, we note that the reaction of  $\text{TeCl}_4$  with  $\text{LiN}(\text{SiMe}_3)_2$  results in reduction to give the tellurium(II) derivative  $\text{Te}[\text{N}(\text{SiMe}_3)_2]_2$ , possibly by a radical process.<sup>25</sup> By contrast, we found that the reaction of  $\text{TeCl}_4$  with  $\text{LiNH}^t\text{Bu}$  in a 1:4 molar ratio in toluene produces  ${}^1\text{BuNTe}(\mu\text{-N}^t\text{Bu})_2\text{TeN}^t\text{Bu}$  (**2c'**) as the major product (41%) together with smaller amounts (17%) of the cyclic tellurium(II) imide  $({}^1\text{BuNTe})_3$ .<sup>14,26</sup> Remarkably, the orange dimer **2c'** can be sublimed at  $75^\circ\text{C}/10^{-4}$  Torr and melts at  $100\text{--}102^\circ\text{C}$  without decomposition. It is also very soluble in organic solvents. Compounds previously formulated as “ $\text{RN}=\text{Te}=\text{NR}$ ” ( $\text{R} = \text{MeCO}, \text{PhSO}_2$ ) are reported to have high melting points and low solubilities.<sup>27</sup> Consequently, these so-called tellurium diimides probably have highly associated structures. It seems likely that the thermal stability of **2c'** is attributable to its dimeric structure, since the corresponding selenium diimide  ${}^1\text{BuN}=\text{Se}=\text{N}^t\text{Bu}$  decomposes slowly at room temperature.<sup>12</sup> In an attempt to kinetically stabilize a monomeric tellurium diimide, the reaction of  $\text{TeCl}_4$  with 4 molar equiv of  ${}^1\text{Bu}_3\text{C}_6\text{H}_2\text{NHLi}$  in toluene at  $-78^\circ\text{C}$  was investigated. However, elemental tellurium was deposited upon warming the reaction mixture to room temperature. The formation of the thermally unstable monomer  ${}^1\text{Bu}_3\text{C}_6\text{H}_2\text{N}=\text{Te}=\text{NC}_6\text{H}_2{}^1\text{Bu}_3$ , which is prohibited by the bulky  ${}^1\text{Bu}_3\text{C}_6\text{H}_2\text{N}$  groups from stabilization through dimerization, is a possible explanation of this observation. The reaction of  $\text{TeCl}_4$  with  $\text{EtNHLi}$  proceeded less cleanly than the corresponding reaction with  ${}^1\text{BuNHLi}$ , and we were unable to isolate pure, crystalline products.

**X-ray Structures of  $\text{RNTe}(\mu\text{-NR}')_2\text{TeNR}$  (**2a**,  $\text{R}' = {}^1\text{Bu}$ ,  $\text{R} = \text{PPh}_2\text{NSiMe}_3$ ; **2b**,  $\text{R}' = {}^i\text{Oct}$ ,  $\text{R} = \text{PPh}_2\text{NSiMe}_3$ ) and  ${}^1\text{BuNTe}(\mu\text{-N}^t\text{Bu})_2\text{TeN}^t\text{Bu}$  (**2c'**).** ORTEP drawings and pertinent bond lengths and bond angles for **2a**<sup>13</sup> and **2c'**<sup>14</sup> were given in the preliminary communications. An ORTEP drawing of the centrosymmetric structure of **2b** is illustrated in Figure 1. The asymmetric unit of **2b** contains two halves of the centrosymmetric dimers. There are two independent molecules of **2b** in the unit cell, but there are no significant differences in the structural parameters for the most important features of these two molecules (see Table 5).

The X-ray analyses of **2a**, **2b**, and **2c'** confirm that these tellurium diimides exist as dimers with a central four-membered  $\text{Te}_2\text{N}_2$  ring in the solid state. There are two major differences between the structures of **2a** and **2b** and that of **2c'**. First, the  $\text{Te}_2\text{N}_2$  rings in **2a** and **2b** are essentially planar whereas that in **2c'** is distinctly folded. Second, the exocyclic imido substituents in **2a** and **2b** adopt a *trans* orientation with respect to the  $\text{Te}_2\text{N}_2$  ring while the terminal  $\text{N}^t\text{Bu}$  groups in **2c'** occupy *cis* positions

(24) Goehring, W.; Weis, G. *Angew. Chem., Int. Ed. Engl.* **1956**, *68*, 687.

(25) Björgvinsson, M.; Roesky, H. W.; Pauer, F.; Stalke, D.; Sheldrick, G. M. *Inorg. Chem.* **1990**, *29*, 5140.

(26) A radical process could account for the formation of  $({}^1\text{BuNTe})_3$ . However, the expected volatile product of such a process (via hydrogen abstraction) is  ${}^1\text{BuNH}_2$ , which is also the major product in the synthesis of **2c'**. A GC-MS study of the volatiles from the 1:4 reaction revealed a complex mixture including  ${}^1\text{BuN}=\text{N}^t\text{Bu}$  ( $m/z$  142).

(27) Markovskii, L. N.; Stukalo, E. O.; Kunitskayo, G. P. *J. Org. Chem. USSR (Engl. Transl.)* **1977**, *13*, 1911.

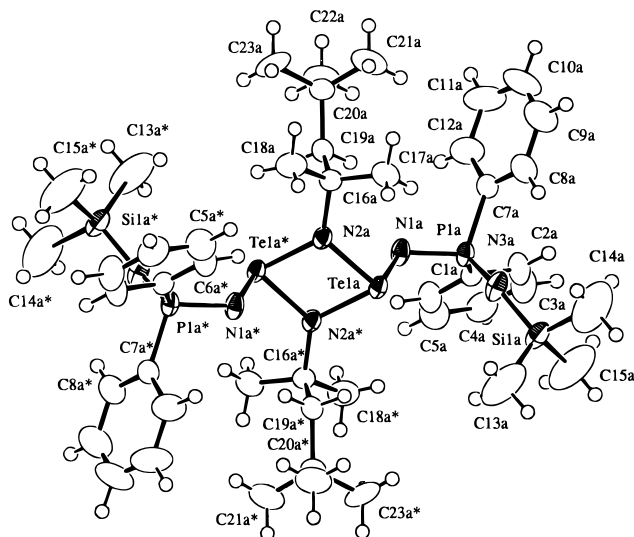


**Figure 1.** ORTEP diagram and atomic numbering scheme for  $RNTe(\mu-N'Oct)_2TeNR$  ( $R = PPh_2NSiMe_3$ ). Only one of the two independent molecules in the unit cell is shown.

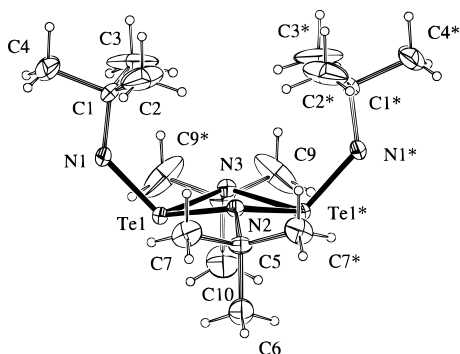


**Figure 2.** ORTEP diagram of  $[BuNTe(\mu-N'Bu)_2TeN'Bu]$ .

**Table 6.** Comparison of Selected Structural Parameters for **2a**, **2b**, and **2c'** (Å; deg)

	<b>2a</b>	<b>2b<sup>a</sup></b>	<b>2c'</b>
Te–N <sub>b</sub> <sup>b</sup>	2.005(5)	2.027(4)	2.080(8)
	2.013(5)	2.022(4)	2.082(8)
Te–N <sub>t</sub> <sup>b</sup>	1.900(5)	1.901(4)	1.876(10)
N <sub>b</sub> TeN <sub>b</sub>	76.5(2)	77.2(2)	75.6(4)
N <sub>b</sub> TeN <sub>t</sub>	104.8(2)	103.0(2)	113.7(5)
N <sub>b</sub> *TeN <sub>t</sub>	97.8(2)	98.8(2)	113.1(5)
TeN <sub>b</sub> Te	103.5(2)	102.7(2)	101.1(6)
Σ∠N <sub>b</sub>	352.4	352.7	342.0 <sup>c</sup>

<sup>a</sup> Mean values for molecules A and B. <sup>b</sup> N<sub>b</sub> = bridging nitrogen; N<sub>t</sub> = terminal nitrogen. <sup>c</sup> Mean value for the two inequivalent N<sub>b</sub> atoms.

(see Figure 2). More subtle differences are apparent from a comparison of the structural parameters of **2a**, **2b**, and **2c'** summarized in Table 6. The bridging Te–N distances of 2.081(8) Å for **2c'** are significantly longer than the mean values of 2.009(5) and 2.025(4) Å for **2a** and **2b**, respectively, while the geometry at the bridging nitrogen atoms is closer to planarity (Σ∠N<sub>b</sub> = 352–353°) in **2a** and **2b** than in **2c'** (Σ∠N<sub>b</sub> = 342°). The exocyclic Te–N bond length of 1.876(10) Å in **2c'** is not significantly different from the values of 1.900(5) and 1.901(4) Å found for **2a** and **2b**, respectively. These bond lengths imply substantial double-bond character,<sup>8,9</sup> but an understanding of the nature of the bonding in these tellurium diimide dimers will require MO calculations on appropriate model compounds.

**Isomerization of 2a and 2b in Solution.** The NMR data for **2a** and **2b** are summarized in Table 1. A freshly prepared solution of **2a** in C<sub>6</sub>D<sub>6</sub> at 25 °C exhibits equally intense singlets

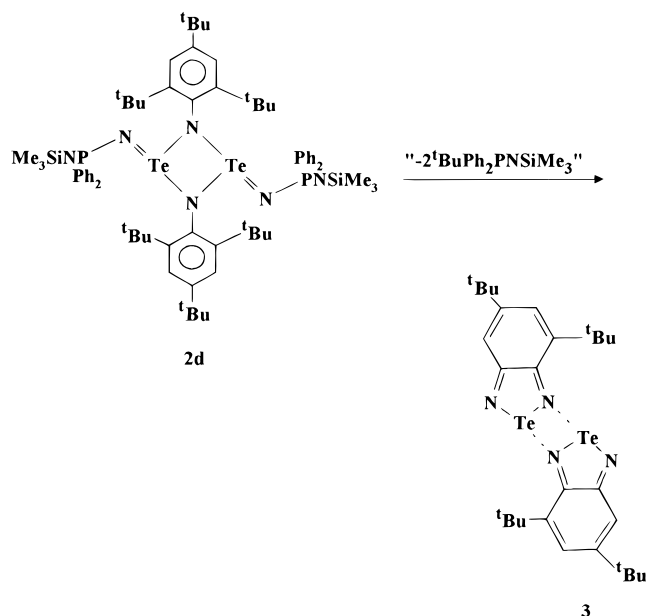
at δ 1.069 and 0.277, attributed to the CMe<sub>3</sub> and SiMe<sub>3</sub> groups, respectively, in addition to the resonances for aromatic protons. Over a period of several hours, two other singlets at δ 1.073 and 0.369, attributed to isomer **2a'**, slowly grow in intensity. Related changes with time are also observed in the <sup>31</sup>P and <sup>125</sup>Te NMR spectra of solutions of **2a** in THF. Thus the <sup>31</sup>P NMR spectrum of pure **2a** in THF exhibits a singlet at δ 14.4 with <sup>125</sup>Te satellites. A second singlet at δ 12.5, which also has <sup>125</sup>Te satellites, slowly develops until its intensity is about half that of the resonance at δ 14.4 after 4 h. The <sup>125</sup>Te NMR spectrum of pure **2a** in THF shows a doublet at δ 1808.2 [<sup>2</sup>J(<sup>31</sup>P–<sup>125</sup>Te) = 131.2 Hz] and a second doublet at δ 1632.4 [<sup>2</sup>J(<sup>31</sup>P–<sup>125</sup>Te) = 109.2 Hz] grows in intensity with time.

Similar behavior is observed for solutions of **2b** when the NMR spectra are monitored over a period of several hours. In this case, the overlap of the multitude of resonances attributable to the –CMe<sub>2</sub>CH<sub>2</sub>CMe<sub>3</sub> groups of the two isomers precludes the unambiguous identification of isomer **2b'** in the <sup>1</sup>H NMR spectrum. However, both the <sup>31</sup>P and <sup>125</sup>Te NMR spectra of **2b** provide evidence for the slow formation of isomer **2b'** in solution. The pertinent NMR data are summarized in Table 1. The <sup>31</sup>P NMR chemical shifts of **2b** and **2b'** are very similar to those of **2a** and **2a'**, respectively. However, in the <sup>125</sup>Te NMR spectrum, the resonance for the minor isomer **2b'** is observed at lower frequency than that for **2b**, which is the opposite of the trend found for **2a** and **2a'**. The explanation of this unexpected reversal is not obvious. In view of the close similarity of the <sup>1</sup>H and <sup>31</sup>P NMR parameters for the pairs of isomers **2a/2a'** and **2b/2b'**, it is proposed that the minor isomers **2a'** and **2b'** exhibit a *cis* arrangement of the exocyclic imido groups as observed in the solid state for the dimer  $[BuNTe(\mu-N'Bu)_2TeN'Bu]$  (**2c'**).<sup>28</sup>

The existence of *cis* and *trans* isomers is well established for the related four-membered rings (R<sub>2</sub>NPNBu)<sub>2</sub>,<sup>29</sup> but the factors that determine the relative stability are not well understood. For example, the *cis* isomer is favored by an increase in the bulk of the exocyclic NR<sub>2</sub> substituents<sup>30,31</sup> whereas the *trans* isomer is favored for ((alkyl)<sub>2</sub>NPNary)<sub>2</sub>, i.e. upon changing the N-substituent from Bu<sup>t</sup> to aryl.<sup>32</sup> There are several possible explanations for the conversion of the *trans* isomers **2a** and **2b** to the corresponding *cis* isomers **2a'** and **2b'** in solution: (a) the existence of a dimer ⇌ monomer equilibrium, (b) pyramidal inversion at one of the two tellurium atoms, or (c) the formation of eight-membered rings. Mechanism a seems unlikely since no exchange between terminal and bridging Bu<sup>t</sup> groups is observed for **2c'**.<sup>14</sup> The selective inversion at *one* tellurium atom is also doubtful. The formation of eight-membered rings (pathway c), which is characterized by a negative activation entropy and has been established for the related *cis*–*trans* isomerization of the four-membered heterocycle (MeP(S)S)<sub>2</sub>,<sup>33</sup> is a reasonable explanation in the

- (28) The <sup>1</sup>H NMR spectrum of a freshly prepared solution of **2c'** in C<sub>7</sub>D<sub>8</sub> at 280 K exhibits two pairs of equally intense singlets (δ 1.68, 1.25 and δ 1.59, 1.28) with relative intensities of ca. 4:1, implying the presence of two isomers. However, the relative amounts of these two isomers do not change significantly within the temperature range 195–370 K. The explanation of these observations will require a detailed multinuclear (<sup>1</sup>H, <sup>15</sup>N, <sup>125</sup>Te) variable-temperature NMR study.
- (29) Keat, R. In *The Chemistry of Inorganic Homo- and Heterocycles*; Haiduc, I., Sowerby, D. B., Eds.; Academic Press: London, 1987; Vol. 2, Chapter 19, p 486.
- (30) Keat, R.; Rycroft, D. S.; Thompson, D. G. *J. Chem. Soc., Dalton Trans.* **1980**, 321.
- (31) Zeiss, W.; Feldt, C.; Weis, J.; Dunkel, G. *Chem. Ber.* **1978**, *111*, 1180.
- (32) Bulloch, G.; Keat, R.; Thompson, D. G. *J. Chem. Soc., Dalton Trans.* **1977**, 99.
- (33) Hahn, J.; Hopp, A.; Borkowsky, A. *Phosphorus, Sulfur, Silicon Relat. Elem.* **1992**, *64/65*, 129.

## Scheme 2



present case. Unfortunately, however, attempts to determine the order and activation parameters for the *cis*–*trans* isomerization process by DNMR methods were thwarted by the decomposition of solutions of **2a** and **2b** over the time period necessary for the VT NMR experiments.

**Synthesis and Structure of (C<sub>6</sub>H<sub>2</sub><sup>t</sup>Bu<sub>2</sub>N<sub>2</sub>Te)<sub>2</sub> (3).** In another attempt to kinetically stabilize a monomeric tellurium diimide by the use of a very bulky group, the reaction of **1** with 2,4,6-<sup>t</sup>Bu<sub>3</sub>C<sub>6</sub>H<sub>2</sub>NHLi was investigated. Surprisingly, the major product of this reaction contained no phosphorus (<sup>31</sup>P NMR spectrum) and exhibited only *two* *tert*-butyl groups and two aromatic protons in the <sup>1</sup>H NMR spectrum. An X-ray structural determination revealed that this compound is 3,5-di-*tert*-butylbenzo-1,2,7-telluradiazole, **3** (*vide infra*). The elimination product Ph<sub>2</sub>P(NSiMe<sub>3</sub>)(NHSiMe<sub>3</sub>) was identified in the <sup>31</sup>P NMR spectrum of the reaction mixture. Thus it is reasonable to infer a reaction pathway similar to that proposed in Scheme 1 for the formation of **2a** and **2b**. In the case of R = 2,4,6-<sup>t</sup>Bu<sub>3</sub>C<sub>6</sub>H<sub>2</sub>, however, the formation of **3** from the hypothetical dimer **2d**<sup>34</sup> must result from intramolecular ring closure and the concomitant cleavage of a C(aryl)–C(CH<sub>3</sub>)<sub>3</sub> bond (see Scheme 2). A related ring closure is observed in the formation of *Se*-chloro-*N*-(4,6-di-*tert*-butyl-2-oxocyclohexa-3,5-dien-1-ylidene)selenamide from the reaction of SeOCl<sub>2</sub> with 2,4,6-<sup>t</sup>Bu<sub>3</sub>C<sub>6</sub>H<sub>2</sub>NH<sub>2</sub> in toluene at reflux.<sup>36</sup> An attempt was made to identify the expected elimination product <sup>t</sup>BuPh<sub>2</sub>PNSiMe<sub>3</sub> by GC-MS, but the only phosphorus-containing product in the reaction mixture that could be identified by this technique was Ph<sub>2</sub>P(NSiMe<sub>3</sub>)(NHSiMe<sub>3</sub>).

The X-ray crystal structure determination of **3** showed that it exists as a weakly associated dimer in the solid state; half of the dimer represents the asymmetric unit. An ORTEP drawing with the atomic numbering scheme is shown in Figure 3, and selected bond distances and bond angles are summarized in

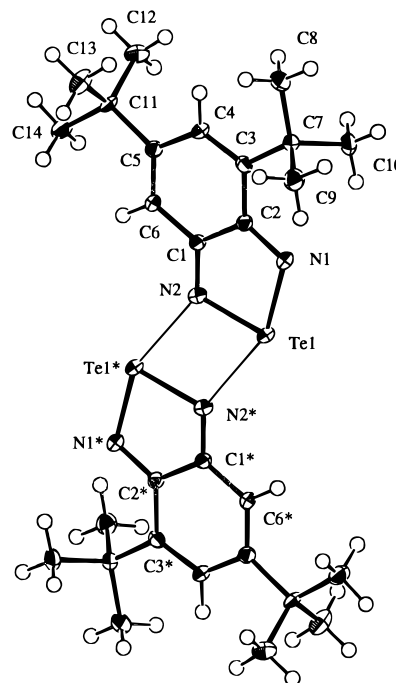
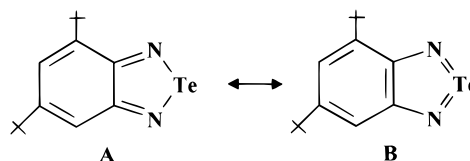


**Figure 3.** ORTEP diagram and atomic numbering scheme for (tBu<sub>2</sub>C<sub>6</sub>H<sub>2</sub>N<sub>2</sub>Te)<sub>2</sub> (**3**).

**Table 7.** Selected Bond Distances (Å) and Bond Angles (deg) for (tBu<sub>2</sub>C<sub>6</sub>H<sub>2</sub>N<sub>2</sub>Te)<sub>2</sub> (**3**)

Te(1)–N(1)	2.006(4)	Te(1)–N(2)	2.002(3)
N(1)–C(2)	1.332(5)	N(2)–C(1)	1.321(5)
C(1)–C(2)	1.477(6)	C(1)–C(6)	1.443(5)
C(2)–C(3)	1.462(6)	C(3)–C(4)	1.366(5)
C(4)–C(5)	1.457(6)	C(5)–C(6)	1.350(6)
N(1)–Te(1)–N(2)	85.8(1)	Te(1)–N(1)–C(2)	108.9(3)
Te(1)–N(2)–C(1)	108.9(3)	N(2)–C(1)–C(2)	118.6(4)
N(2)–C(1)–C(6)	121.3(4)	C(2)–C(1)–C(6)	120.0(4)
N(1)–C(2)–C(1)	117.7(4)	N(1)–C(2)–C(3)	123.5(4)
C(1)–C(2)–C(3)	118.8(4)	C(2)–C(3)–C(4)	116.8(4)
C(2)–C(3)–C(7)	120.9(4)	C(4)–C(3)–C(7)	122.3(4)
C(3)–C(4)–C(5)	124.6(4)	C(4)–C(5)–C(6)	119.8(4)
C(4)–C(5)–C(11)	116.7(4)	C(6)–C(5)–C(11)	123.5(4)
C(1)–C(6)–C(5)	119.8(4)		

Table 7. The intramolecular Te–N distances of 2.002(3) and 2.006(4) Å are slightly shorter than the reported average distances of 2.02 Å for the parent 1,2,5-telluradiazole<sup>37</sup> and phenanthro[9,10-*c*]-1,2,5-telluradiazole.<sup>37</sup> The bond angle of 85.8(1)° at tellurium is comparable to the values of 82.5(5) and 84.3(3)° found for the other telluradiazoles.<sup>37,38</sup> These data and the pattern of C–C and C–N bond distances (see Table 6) indicate that the tellurium(II) resonance form **A** is a more important contributor than **B** [tellurium(IV)] to the overall structure of **3**.



There are strong intermolecular attractions in **3** with Te–N distances of 2.628(4) Å; cf. 3.70 Å for the sum of the van der Waals radii of these atoms. This separation can be compared

(34) The formation of **3** from the putative monomer <sup>t</sup>Bu<sub>3</sub>C<sub>6</sub>H<sub>2</sub>N=Te=NPh<sub>2</sub>NSiMe<sub>3</sub> by the elimination of <sup>t</sup>BuPh<sub>2</sub>PNSiMe<sub>3</sub> seems less likely in view of the known preference of chalcogen diimides for a *cis,trans* geometry (see Scheme 1).<sup>35</sup>

(35) Wrackmeyer, B.; Distler, B.; Gerstmann, S.; Herberhold, M. Z. *Naturforsch.* **1993**, *48B*, 1307.

(36) Roesky, H. W.; Weber, K.-L.; Seseke, U.; Pinkert, W.; Noltemeyer, M.; Clegg, W.; Sheldrick, G. M. *J. Chem. Soc., Dalton Trans.* **1985**, 565.

(37) Bertini, V.; Dapporto, P.; Lucchesini, F.; Sega, A.; De Munno, A. *Acta Crystallogr.* **1984**, *C40*, 653.

(38) Neidlein, R.; Knecht, D. Z. *Naturforsch.* **1987**, *42B*, 84.

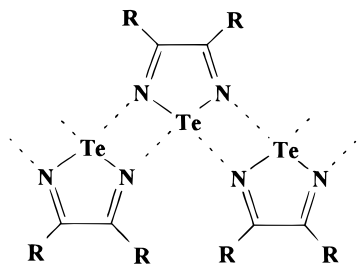


**Figure 4.** Schematic representation of the polymeric structure of 1,2,5-telluradiazoles.

with the average values of 2.764(6) and 2.834 Å reported for 1,2,5-telluradiazole<sup>37</sup> and phenanthro[9,10-*c*]-1,2,5-telluradiazole,<sup>38</sup> respectively. The properties of **3** are in distinct contrast to those of the parent 1,2,5-telluradiazole, which is a high-melting solid with poor solubility in organic solvents.<sup>39</sup> Compound **3** melts sharply at 207–208 °C and can be recrystallized from pentane. Significantly, there are no interactions between dimeric units in **3** whereas the other 1,2,5-telluradiazoles exist as either planar<sup>37</sup> or ladder-type<sup>38</sup> polymers (see Figure 4). Inspection of the packing diagram for **3** (see Figure 5) suggests that the bulky *tert*-butyl groups prevent further association of the dimeric units in this case.

**Conclusion.** The reaction of amidolithium reagents RNHLi (R = <sup>t</sup>Bu, <sup>o</sup>Oct) with the readily prepared PN<sub>2</sub>Te heterocycle **1** unexpectedly produces excellent yields of the tellurium diimides **2a** and **2b**, which are stabilized by dimerization to give Te<sub>2</sub>N<sub>2</sub> ring systems with the NR (R = <sup>t</sup>Bu, <sup>o</sup>Oct) groups in the bridging positions. In the specific case of R = <sup>t</sup>Bu<sub>3</sub>C<sub>6</sub>H<sub>2</sub>, this reaction produces a telluradiazole which, unlike known 1,2,5-telluradiazoles, exists as a discrete dimer in the solid state. In the solid state, **2a** and **2b** are isolated as the *trans* isomers, but slow conversion to the corresponding *cis* isomers occurs in solution. By contrast, the dimer <sup>t</sup>BuNTe( $\mu$ -N<sup>t</sup>Bu)<sub>2</sub>TeN<sup>t</sup>Bu, prepared by

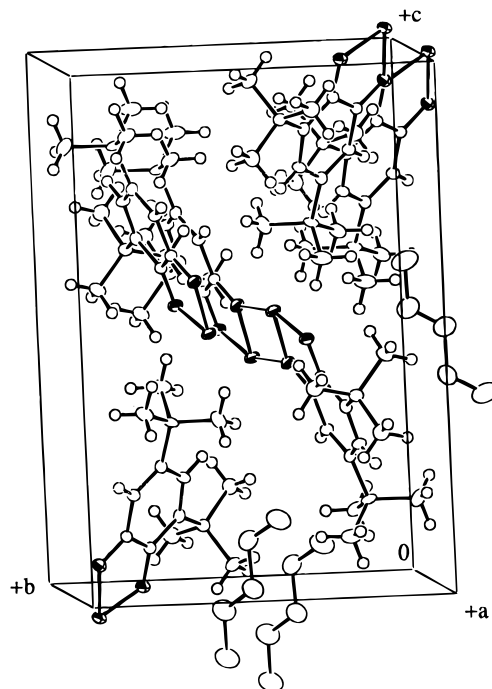


**Figure 5.** Packing diagram for (<sup>t</sup>Bu<sub>2</sub>C<sub>6</sub>H<sub>2</sub>N<sub>2</sub>Te)<sub>2</sub> (**3**).

the reaction of TeCl<sub>4</sub> with 4 equiv of <sup>t</sup>BuNHLi, exists as the *cis* isomer in the solid state.

**Acknowledgment.** We thank the NSERC (Canada) for financial support.

**Supporting Information Available:** Tables giving experimental crystallographic details, bond lengths, bond angles, torsion angles, and anisotropic displacement parameters for non-hydrogen atoms and atomic coordinates for hydrogen atoms of **2b** and **3** (23 pages). Ordering information is given on any current masthead page.

(39) Bertini, V.; Lucchesini, F.; De Munno, A. *Synthesis* **1982**, 681.